



**AALBORG UNIVERSITY**  
DENMARK

**Aalborg Universitet**

## **Decentralized Model Predictive Control of DC Microgrids with Constant Power Load**

Karami, Zeinab; Shafiee, Qobad; Khayat, Yousef; Yaribeygi, Meysam; Dragicevic, Tomislav; Bevrani, Hassan

*Published in:*

IEEE Journal of Emerging and Selected Topics in Power Electronics

*DOI (link to publication from Publisher):*

[10.1109/JESTPE.2019.2957231](https://doi.org/10.1109/JESTPE.2019.2957231)

*Publication date:*

2019

*Document Version*

Accepted author manuscript, peer reviewed version

[Link to publication from Aalborg University](#)

*Citation for published version (APA):*

Karami, Z., Shafiee, Q., Khayat, Y., Yaribeygi, M., Dragicevic, T., & Bevrani, H. (2019). Decentralized Model Predictive Control of DC Microgrids with Constant Power Load. *IEEE Journal of Emerging and Selected Topics in Power Electronics*. <https://doi.org/10.1109/JESTPE.2019.2957231>

### **General rights**

Copyright and moral rights for the publications made accessible in the public portal are retained by the authors and/or other copyright owners and it is a condition of accessing publications that users recognise and abide by the legal requirements associated with these rights.

- ? Users may download and print one copy of any publication from the public portal for the purpose of private study or research.
- ? You may not further distribute the material or use it for any profit-making activity or commercial gain
- ? You may freely distribute the URL identifying the publication in the public portal ?

### **Take down policy**

If you believe that this document breaches copyright please contact us at [vbn@aub.aau.dk](mailto:vbn@aub.aau.dk) providing details, and we will remove access to the work immediately and investigate your claim.

# Decentralized Model Predictive Control of DC Microgrids with Constant Power Load

Zeinab Karami, Qobad Shafiee, *Senior Member, IEEE*, Yousef Khayat, *Student Member, IEEE*, Meysam Yaribeygi, Tomislav Dragicevic, *Senior Member, IEEE*, Hassan Bevrani, *Senior Member, IEEE*

**Abstract**—This paper introduces a decentralized model predictive controller (DMPC) to ensure power sharing and regulate dc bus voltage in dc microgrids (MGs) with constant power load (CPL). The proposed method replaces the conventional primary layer of dc MGs, i.e., inner loops and droop control, with a single optimal controller. A predictive *automatic* model of the system is realized for prediction purposes and to be used in the cost function. The control objectives are then incorporated in the cost function to attain an optimal state switching in each sampling time, hence regulating dc bus voltage and accurate sharing of current among the MG. The proposed solution provides the system with a fast dynamic response and zero steady state error. The effectiveness of proposed control is verified via hardware-in-the-loop real time experiments, and the results are compared with the conventional primary control.

**Index Terms**—Automatic model, constant power load, current sharing, DC microgrid, model predictive control.

## I. INTRODUCTION

**DC** MODERN power systems and MGs are a promising solution, which not only improve the utility system efficiency and reliability, but also they simplify the integration of renewable and energy storage systems (ESSs) due to the inherently dc output of many of renewable energy systems (RESs) technologies [1], [2]. Additional features of dc systems are their simplicity to control as there are no synchronization concerns, reactive power flows, and phase unbalances [3]. These features have led to a lot of interest in dc distribution systems and dc MGs.

A large majority of end-users in dc MGs are electronic loads that employ converters for power conditioning and voltage regulation. Active regulation capability of constant power loads (CPLs) extracts steady power even under dc voltage variation at the dc bus side [4]. A challenging characteristic of CPLs is their input negative impedance feature. This characteristic may lead the system to which it is connected towards instability. Different solutions have been suggested to deal with this challenge such as: 1) passive or active damping of source side impedance [5], 2) active damping of the CPL's impedance [6], [7], and 3) utilizing effective (linear and nonlinear) control strategies [8]–[10]. Passive damping of source side impedance requires installation of a passive component which increases the size and losses of the system [7]. While, for active damping one can actively control the power electronic converter at

the source side [7], [10]–[12]. However, employing active converters merely for stabilizing is too costly and is not justifiable.

In addition to the above mentioned challenges, appropriate voltage regulation (VR) as well as current sharing (CS) among distributed generation units (DGUs) in the presence of the CPLs consideration. Active current-sharing techniques involve a centralized control structure to provide a reference current [13], [14]. These methods have two main limitations: 1) high-speed communication is required, 2) single point of failure feature which leads to lower reliability of the system [15]. To overcome these limitations, decentralized control methods have been widely used for suitable power sharing in DC MGs [16]–[18].

A droop mechanism is often used to provide current sharing and output voltage regulation [19]. In such a mechanism, performance depends on the amount of droop coefficient. Small droop gains result in a proper voltage regulation but inaccurate current sharing and vice versa. To deal with disadvantages of droop control, different control approaches have been introduced in the literature [20]–[22]. An adaptive droop control method is proposed in [23], which minimizes the circulating current and improves the current sharing between the converters based on an instantaneous virtual resistance. In [24], an automatic droop control method is presented based on a comprehensive investigation of the dc MG characteristics where the droop gains are tuned automatically according to the load current without need of any communication network.

In the previously mentioned droop control strategies, a common technique used for voltage and current control is the proportional-integral (PI) controller. PI tuning is frequently necessary for each perturbation due to the high variability and stochastic nature of solar energy in MGs which leads to the increased complexity of the system. In addition to the major problem associated with the PI controller, it is the fact that PI is a linear controller while all power electronics systems are mostly nonlinear. Therefore, tuning this type of linear controllers getting complicated, due to the inherent nonlinearity in the converters and the increasing nonlinearity behavior in the presence of the CPLs. While, model predictive control (MPC) method accounts for nonlinear dynamics, uncertainties and constraints of the system. Inspired by the deficiencies of the state-of-the-art dc MG stabilization approaches summarized above, direct MPC approaches gains popularity for these systems [25]. MPC is an optimal control method that aims at solving an optimization problem over a prediction horizon at each sampling step. The length of the prediction horizon is chosen considering the precision of system model [25]. Predictive control presents numerous advantages that make

The following authors are with the Smart/Micro Grids Research Center, University of Kurdistan, Sanandaj 66177-15175, Kurdistan, Iran. (e-mails: zeinab.karami@eng.uok.ac.ir, q.shafiee@uok.ac.ir, y.khayat@eng.uok.ac.ir, bevrani@uok.ac.ir).

M. Yaribeygi is with the EE Dept. of K. N. Toosi University of Technology, Iran. (e-mail: yaribeygi@email.kntu.ac.ir).

T. Dragicevic is with the Department of Energy Technology, Aalborg University, Aalborg, DK, 9220, Denmark (e-mail: tdr@et.aau.dk).

it appropriate for power converter control due to taking into account constraints, and nonlinearities [26]. Different types of MPC strategies have been recently applied to MGs for various control purposes [27], [28], as well as dynamic stabilization of dc MGs [29]–[34].

This paper presents a decentralized model predictive controller (DMPC) to ensure power sharing and regulate dc bus voltage in dc MGs with CPL. The proposed method replaces the conventional primary layer of dc MGs, i.e., inner loops and droop control, with a single optimal controller. An automatic model of dc MGs is derived in order to formulate a cost function for the proposed DMPC. The discrete-time model is derived such that it precisely predicts the system behavior. Thus, the designed DMPC is applicable to the whole operating regime, rather than just to a particular operating point. Using real-time experimental studies, efficiency of the proposed control framework comparing with the conventional primary control is examined under different scenarios. The contributions of this paper can be summarized as follows:

- The proposed framework takes the duty of inner (current/voltage) loops as well as the droop mechanism in the conventional primary control of dc MGs using a single optimal controller. The proposed decentralized controller provides accurate voltage regulation and current sharing with no need of digital communication.
- It introduces an augmented automatic model taking into account all switching modes. This gives the possibility of using a simple hybrid MPC instead of a nonlinear one. The model obtains integral modes which results in elimination of disturbances and tracking of signals without error. Using the augmented model, the proposed DMPC provides appropriate transient and steady state performance.
- The proposed DMPC takes into account the nonlinear dynamics of dc MGs in the presence of CPLs and gives a systematic technique of dealing with constraints on inputs.

The rest of the paper is organized as follows: In Section II, the nonlinear averaged and automatic dynamic models of the converter is summarized. The DMPC design procedure is introduced in Section III. Section IV provides real-time experimental studies verifying effectiveness of the DMPC framework. Finally, the paper is concluded in Section V.

## II. MATHEMATICAL MODEL OF A DC MICROGRID

Nowadays, many applications such as aircraft, aerospace, Marin and Naval systems utilize the concept of dc MG due to dc system features e.g., improved efficiency, flexibility, and reliability through providing redundancy. A typical dc MG contains a number of DGUs and loads all connected to a common dc bus. DGUs include a number of RESs and ESSs interfaced by power electronic converters. Fig. 1, illustrates general configuration of a dc MG. In this paper, an islanded dc MG with four photovoltaic (PV) sources supporting a CPL is considered. In formulation and procedure design, without losing generality, we assume that boost converters are used as dc-dc converters. However, one can use any type of the

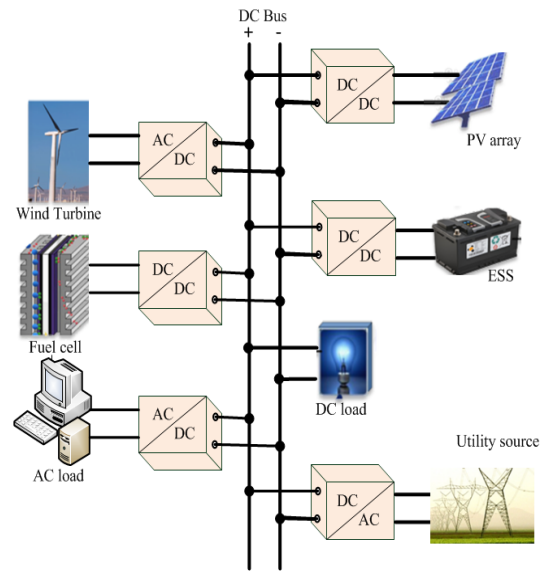


Fig. 1: General configuration of a dc microgrid with multiple sources.

converters in the system. Fig. 2, shows general configuration of one DG inside a dc MG, e.g., a PV, connected to a dc-dc converter interfaced with a CPL. State space model of a dc-dc boost converter with any type load such as  $Z$  considering the inductor current  $i_L$ , capacitor voltage  $v_c$  and input voltage  $v_{in}$ , is expressed as [35].

$$\dot{i}_L(t) = \tilde{d} \left[ -\frac{R_L}{L} - \frac{Z}{L(Z+R_c)} \right] i_L(t) - \tilde{d} \frac{Z}{L(Z+R_c)} v_c(t) + \frac{Z}{L(Z+R_c)} (R_c i_L(t) + v_c(t)) u(t) + \tilde{d} \frac{v_{in}(t)}{L} \quad (1)$$

$$\dot{v}_c(t) = \tilde{d} \frac{Z}{C_f(Z+R_c)} i_L(t) - \frac{1}{C_f(Z+R_c)} v_c(t) - \frac{Z}{C_f(Z+R_c)} i_L(t) u(t) \quad (2)$$

$$v_o(t) = \tilde{d} \frac{Z R_c}{Z+R_c} i_L(t) + \frac{Z}{Z+R_c} v_c(t) - \frac{Z R_c}{Z+R_c} i_L(t) u(t) \quad (3)$$

$$u(t) = \begin{cases} 1 & S = 1 \\ 0 & S = 0 \end{cases} \quad (4)$$

$$\tilde{d}(t) = \begin{cases} 1 & u(t) \geq 0 \text{ and } i_L(t) > 0 \\ 0 & u(t) = 0 \text{ and } i_L(t) = 0 \end{cases} \quad (5)$$

where  $L$  is the inductor with  $R_L$  representing the inductor equivalent series resistance,  $C_f$  is the output capacitor with  $R_c$  representing its equivalent series resistance,  $u(t)$  is the input of the system,  $S = 1$  means the switch is ON and  $S = 0$  indicates the switch is OFF. In discontinuous conduction mode (DCM) operation, the inductor current returns to zero in every switching cycle, thus the auxiliary binary variable  $\tilde{d}$  is introduced to derive a model that describes the operation of the converter either in DCM (when  $\tilde{d} = 0$ ) or continuous conduction mode (CCM) (when  $\tilde{d} = 1$ ).

Taking into account the inductor current, a dc-dc boost converter, can be classified into two models: averaged and automatic models [32], [33]. The modelling procedure for a boost converter is expressed as follows.

## A. Averaged Model of a Boost Converter

1) *Continuous-Time Model:* Circuit schematic of a DGU with a CPL is shown in Fig. 3. There exist two different dynamics regarding the switching state of dc-dc boost converter in averaged model. As shown in Fig. 3, when the switch is ON (Fig. 3a) energy is stored in the inductor. While, once the switch is OFF (Fig. 3b) the inductor is connected to the output and energy is released through it to the load. The following nonlinear state space representation describes the dynamics of the system based on an averaged model by using the circuit laws:

$$\frac{di_{Li}(t)}{dt} = (1 - S) \left( -\frac{R_{Li}}{L_i} i_{Li}(t) - \frac{1}{L_i} v_{oi}(t) + \frac{1}{L_i} v_{si}(t) \right) + S \left( -\frac{R_{Li}}{L_i} i_{Li}(t) + \frac{1}{L_i} v_{si}(t) \right) \quad (6)$$

$$\frac{dv_{oi}(t)}{dt} = (1 - S) \left( \frac{1}{C_{oi}} i_{Li}(t) - \frac{P}{C_{oi} v_{oi}^2} v_{oi}(t) \right) + S \left( -\frac{P}{C_{oi} v_{oi}^2} v_{oi}(t) \right) \quad (7)$$

Briefly:

$$\dot{x}(t) = \begin{cases} A_{1i}x(t) + B_i v_s(t) & S = 1 \\ A_{2i}x(t) + B_i v_s(t) & S = 0 \end{cases} \quad y(t) = C_i x(t) \quad (8)$$

where  $x(t) = [i_L(t) \ v_o(t)]$  is the state vector, inductor current and capacitor voltage respectively,  $u(t) = v_{si}(t)$  and  $v_{si}(t)$  is input voltage of power supply which is equal to nominal voltage of PV array  $i$ , for  $i = 1, \dots, 4$ ,  $y(t)$  is the output of the system which here is equal to the output voltage of dc bus, i.e.,  $(v_{oi})$  which is considered equal to voltage  $v_{C_{oi}}$ .  $C_{oi}$  is the output capacitor filter,  $R_{Li}$  is resistance of input inductor  $L_i$ ,  $P$  is power load,  $R_{Line_i}$  is line resistance,  $S$  and  $D$  (diode) are the two power switches where  $S$  is the controllable (MOSFET or IGBT), and  $D$  is the uncontrollable switch. Matrices  $A_{1i}$ ,  $A_{2i}$ ,  $B_i$  and  $C_i$  are calculated as follows:

$$A_{1i} = \begin{bmatrix} \frac{-R_{Li}}{L} & 0 \\ 0 & \frac{-P}{C_{oi} v_{oi}^2} \end{bmatrix}, A_{2i} = \begin{bmatrix} \frac{-R_{Li}}{L_i} & \frac{-1}{L_j} \\ \frac{1}{C_{oi}} & \frac{-P}{C_{oi} v_{oi}^2} \end{bmatrix}, \quad (9)$$

$$B_i = \begin{bmatrix} \frac{1}{L_i} & 0 \end{bmatrix}^T, C_i = \begin{bmatrix} 0 & 1 \end{bmatrix}$$

In this case, the averaged model can be calculated as follows:

$$\dot{x}(t) = S(A_{1i}x(t) + B_{1i}v_{si}) + (1 - S)(A_{2i}x(t) + B_{2i}v_{si}) \quad (10)$$

$$y(t) = C_i x(t)$$

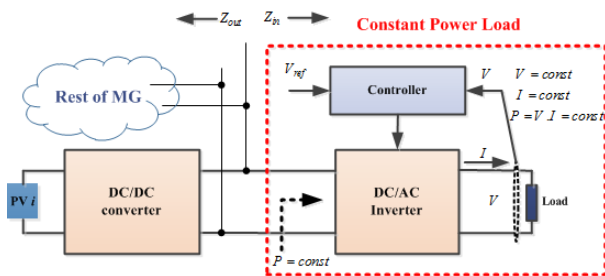


Fig. 2: Schematic diagram of a dc-dc converter with a CPL.

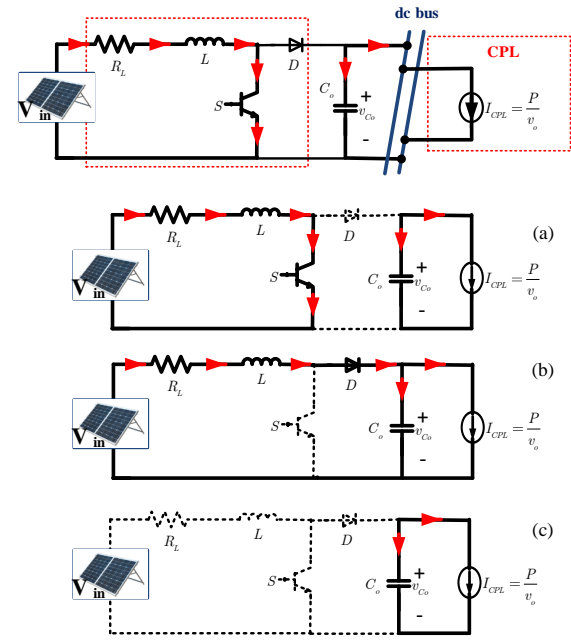


Fig. 3: Circuit schematic of a DG in a dc MG interfaced with CPL as well as operating modes of a dc-dc boost converter for averaged and automatic models: (a) mode 1, (b) mode 2, and (c) mode 3.

2) *Discrete-Time Model:* There are three different dynamic modes in regards to the switch position of a dc-dc boost converter in discrete time averaged model:

1) when the switch  $S$  is ON (see Fig. 3a), energy is stored in the inductor,

2) when the switch  $S$  is OFF (see Fig. 3b), the inductor is connected to the output and energy is released through it to the load.

3) When the switch  $S$  remains OFF and  $i_L(t) = 0$ , in other words, both switches  $S$  and  $D$  are OFF; the topology is reduced to the mesh formed by the capacitor  $C_{oi}$  and the CPL (see Fig. 3c). In this case, the converter operates in DCM. The equations of different modes using circuit law are as following:

$$x(k+1) = \begin{cases} (I + A_{1i}T_s)x(k) + BT_s v_{si}(k), & S = 1 \\ (I + A_{2i}T_s)x(k) + BT_s v_{si}(k), & S = 0 \& i_{Li}(k) > 0 \\ (I + A_{3i}T_s)x(k) & S = 0 \& i_{Li}(k) = 0 \end{cases} \quad (11)$$

where  $A_{3i}$  is as follows:

$$A_{3i} = \begin{bmatrix} 0 & 0 \\ 0 & -\frac{P}{C_{oi} v_{oi}^2} \end{bmatrix} \quad (12)$$

## B. Automatic Model of a Boost Converter

1) *Continuous-Time Model:* Unlike the presented averaged model, in the automatic model the inductor current situation in each sampling time is taken into account in addition to the switching modes. As shown in Fig. 3, boost converter has three operational modes for automatic model in continues time. The following nonlinear state space equations describe the dynamics of the system based on automatic model by using circuit laws [34].

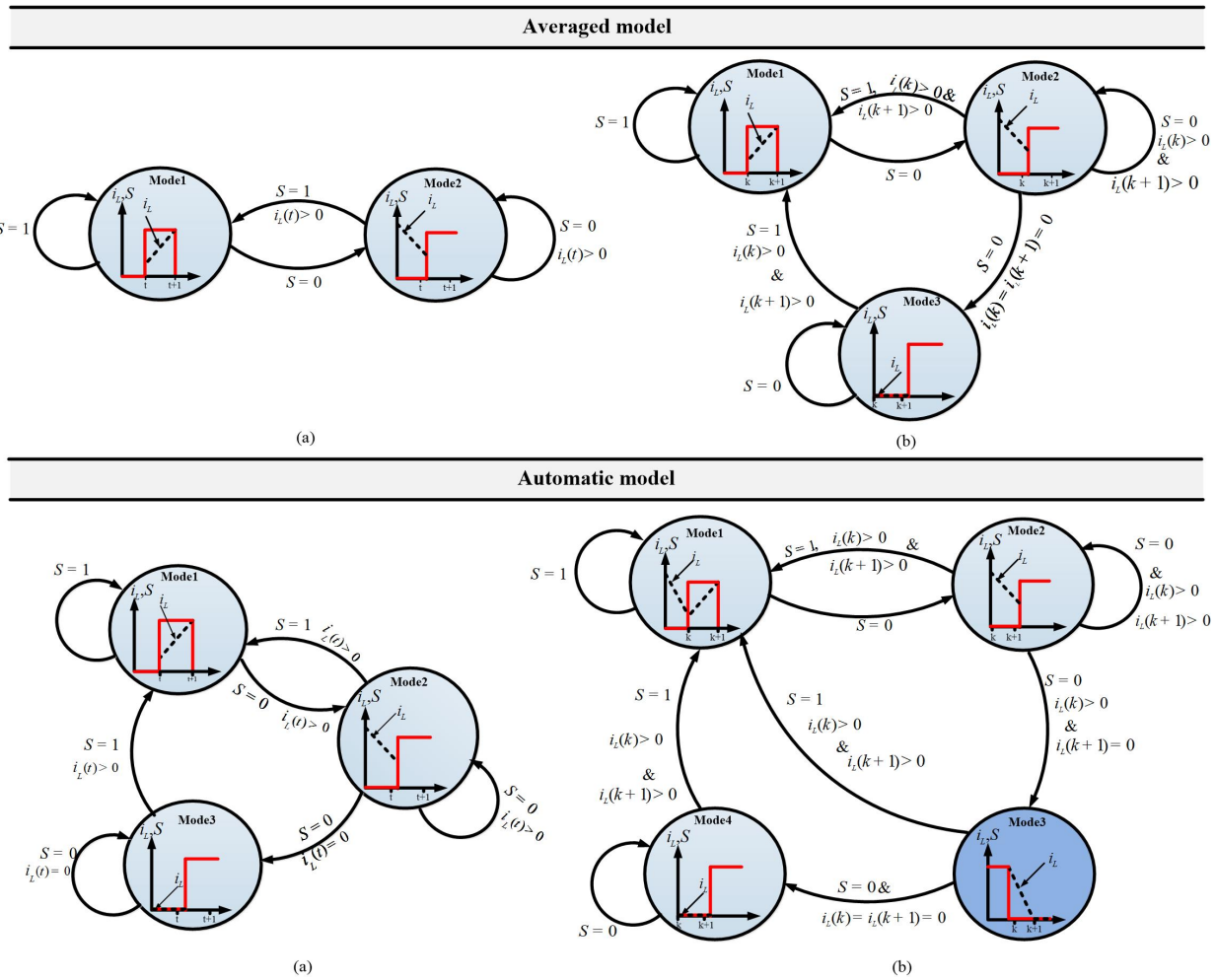


Fig. 4: Possible averaged and automatic modes in continuous and discrete times for a dc-dc boost converter, (a) continuous time (b) discrete time.

- 1) When the switch  $S$  is ON and inductor current increases (i.e.,  $i_{L_i}(t) \uparrow$ ). In this mode energy is stored in the inductor and its current increases (Fig. 3a).
- 2) When the switch  $S$  is OFF and inductor current decreases (i.e.,  $i_{L_i}(t) \downarrow$ ). The inductor is connected to the output and energy is released through it toward the common bus (Fig. 3b).
- 3) When the switch  $S$  remains OFF and  $i_{L_i}(t) = 0$ , in other words both switches  $S$  and  $D$  are OFF. In this case, the converter operates in DCM (Fig. 3c). The equations of the above mentioned modes using the circuit law are as following:

$$\dot{x}(t) = \begin{cases} A_{1i}x(t) + B_i v_{si}(t) & S = 1 \\ A_{2i}x(t) + B_i v_{si}(t) & S = 0 \text{ \& } i_{L_i}(t) > 0 \\ A_{3i}x(t) & S = 0 \text{ \& } i_{L_i}(t) = 0 \end{cases}$$

$$y(t) = C_i x(t) \quad (13)$$

2) *Discrete-Time Model:* The continuous-time equations of this model as given in (13) is discretized using the Euler approximation approach as:

$$\frac{dx(t)}{dt} = \frac{x(k+1) - x(k)}{T_s} \quad (14)$$

Accordingly, the automatic discrete time model of the studied system with one unit and CPL:

$$x(k+1) = \begin{cases} G_{1i}x(k) + F_i v_{si}(k), & S = 1 \\ G_{2i}x(k) + F_i v_{si}(k), & S = 0 \text{ \& } i_{L_i}(k+1) > 0 \\ G_{3i}x(k), & S = 0 \text{ \& } i_{L_i}(k+1) = 0 \end{cases}$$

$$y(k) = H_i x(k) \quad (15)$$

where  $G_{1i} = I + A_{1i}T_s$ ,  $G_{2i} = I + A_{2i}T_s$ , and  $G_{3i} = I + A_{3i}T_s$ . Furthermore,  $I$  is the identity matrix,  $F_i = B_i T_s$  and  $H_i = C_i$  with dimension two and  $T_s$  is the sampling time. After discretization, the automatic model can operate in the following four different modes.

**Mode 1.** When  $S = 1$ ,  $i_{L_i}(k) > 0$  and  $i_{L_i}(k+1) > 0$ , i.e., the inductor current is positive and the switch is ON for the whole sampling interval. This state space model can be written as following:

$$x(k+1) = G_{1i}x(k) + F_i v_{si}(k)$$

$$i_{L_i}(k+1) = \left(1 - \frac{T_s R L_i}{L_i}\right) i_{L_i}(k) + \frac{T_s}{L_i} v_{si}$$

$$v_{oi}(k+1) = \frac{T_s}{C_{oi}} i_{oi}(k) + v_{oi}(k) \quad (16)$$

**Mode 2.** When  $S = 0$ ,  $i_{L_i}(k) > 0$  and  $i_{L_i}(k+1) > 0$ , i.e.,

the inductor current is positive and the switch is OFF for the whole sampling interval, which its deferential equation is as:

$$\begin{aligned} x(k+1) &= G_{2i}x(k) + F_i v_{si}(k) \\ i_{Li}(k+1) &= \left(1 - \frac{T_s R_{Li}}{L_i}\right) i_{Li}(k) - \frac{T_s}{L_i} v_{oi}(k) + \frac{T_s}{L_i} v_{si} \\ v_{oi}(k+1) &= \frac{T_s}{C_{oi}} (i_{Li}(k) - i_{oi}(k)) + v_{oi}(k) \\ i_{oi}(k+1) &= i_{Li}(k+1) - \frac{C_{oi}}{T_s} (v_{oi}(k+2) - v_{oi}(k+1)) \end{aligned} \quad (17)$$

**Mode 3.** When  $S = 0$ ,  $i_{Li}(k) > 0$  and  $i_{Li}(k+1) = 0$ , i.e., the inductor current reaches zero during the sampling interval, while the switch is OFF, in the other word:

$$\begin{aligned} i_{Li}(k+1) &= \left(\frac{\tau_1}{T_s} \left(1 - \frac{T_s R_{Li}}{L_i}\right) + \frac{\tau_2}{T_s}\right) i_{Li}(k) - \frac{\tau_1}{L_i} v_{oi}(k) \\ v_{oi}(k+1) &= \frac{\tau_1}{C_{oi}} i_{Li}(k) + \left(\frac{\tau_1}{T_s} + \frac{\tau_2}{T_s}\right) \left(1 - \frac{T_s}{C_{oi}}\right) i_{oi}(k) \\ v_{oi}(k+1) &= \frac{\tau_1}{C_{oi}} i_{Li}(k) + \left(\frac{\tau_1 + \tau_2}{T_s}\right) - \left(\frac{\tau_1 + \tau_2}{C_{oi}}\right) i_{oi}(k) \end{aligned} \quad (18)$$

where  $T_s = \tau_1 + \tau_2$ , therefore the value  $v_{oi}(k+1)$  is calculated from equation (20).

$$v_{oi}(k+1) = \frac{\tau_1}{C_{oi}} i_{Li}(k) + 1 - \frac{1}{C_{oi}} i_{oi}(k) \quad (19)$$

**Mode 4.** When  $S = 0$ ,  $i_{Li}(k) = i_{Li}(k+1) = 0$ , i.e., the inductor current is zero and the switch is OFF for the whole sampling interval, as follows:

$$\begin{aligned} x(k+1) &= G_{3i}x(k) \quad S = 0 \quad i_{Li}(k) = i_{Li}(k+1) = 0 \\ v_{oi}(k+1) &= v_{oi}(k) - \frac{T_s}{C_{oi}} i_{oi}(k) \\ i_{oi}(k+1) &= \frac{C_{oi}}{T_s} (v_{oi}(k+2) - v_{oi}(k+1)) \end{aligned} \quad (20)$$

Fig. 4 shows the conversion modes from one fashion to another in continuous and discrete time of averaged and automatic models in a cycle for a dc-dc boost converter. As can be seen in Fig. 4(b), an operational mode (mode 3) is added to the automatic model in discrete time. The equations discrete time of this model can be explained as follow:

$$x(k+1) = G_{4i}x(k) + \frac{\tau_1}{T_s} F_i v_{si}(k) \quad (21)$$

where  $G_{4i} = (1/T_s)(\tau_1 G_{2i} + \tau_2 G_{3i})$ ,  $T_s = \tau_1 + \tau_2$  and  $\tau_1$  denotes the time instant within the sampling interval, when the inductor current reaches zero. Mode transitions are specified by conditions, such as the switch position and the value of the current. To visualize the different modes and the transitions from one mode to the other, a binary variable ( $u$ ) denoting the switch position is introduced, where  $S = 1$  refers to the switch  $S$  being ON, and  $S = 0$  to the switch being OFF [34].

### C. Augmented Automatic Model

Discrete-time state-space models can be used to formulate the predictive control problem. The main stability-related theoretical results of MPC stems from a state-space formulation that can easily apply to non-linear processes and be used for single-variable and multi-variable processes. This paper

utilizes a discrete automatic model in the prediction and design procedure, where all switching modes of the converter are taken into account (equations (15) and (21)). This gives the possibility of using a simple hybrid MPC instead of a nonlinear one.

Notice that in (15) and (21)  $v_{si}(k)$  is considered as input signal. Thus, the model should be changed to suit the design purpose as in which an integrator is embedded. An incremental state-space model can also be used if the model input is the control increment  $\Delta v_{si}(k)$  instead of the control signal  $v_{si}(k)$ . This model is called the augmented model which used in the design of predictive control and is obtained as follows:

$$\begin{aligned} X(k+1) &= \begin{cases} \bar{G}_{1i}X(k) + \bar{F}_i \Delta v_{si}(k), \\ \bar{G}_{2i}X(k) + \bar{F}_i \Delta v_{si}(k), \\ \bar{G}_{3i}X(k), \\ \bar{G}_{4i}X(k) + \frac{\tau_1}{T_s} \bar{F}_i \Delta v_{si}(k) \end{cases} \\ y(k) &= \bar{H}_i X(k) \end{aligned} \quad (22)$$

where  $\Delta x$ , and  $\Delta v_{si}(k)$  are differences of the states, and the input vectors respectively, and matrices  $X(k)$ ,  $\bar{G}_{mi}$ ,  $\bar{F}_i$ , and  $\bar{H}_i$  are calculated as follows:

$$\begin{aligned} X(k) &= \begin{bmatrix} \Delta x(k) & y(k) \end{bmatrix}^T, \bar{G}_{mi} = \begin{bmatrix} G_{mi} & O^T \\ H_i G_{mi} & I_{q \times q} \end{bmatrix} \\ \bar{F}_i &= \begin{bmatrix} F_i & H_i F_i \end{bmatrix}^T, \bar{H}_i = \begin{bmatrix} 0 & I_{q \times q} \end{bmatrix} \end{aligned}$$

where  $m = 1, \dots, 4$  and in matrix  $\bar{G}_{mi}$ ,  $O^T$  is zero vector with appropriate dimension ( $q \times n$ ) that  $n$  is the dimension of the state variable vector, and  $q$  is the number of outputs, that  $q$  integrators are embedded in the augmented model.

## III. DMPC DESIGN PROCEDURE

Droop control is an effective solution to share power among DGUs in a dc MG as well as to regulate the bus voltage. Though, it is realized in a decentralized and communication free approach, its steady state deviations is a major problem regarding to the power quality indices. In contrast with the conventional droop mechanism, the steady state deviations are eliminated in the proposed DMPC while providing voltage regulation and accurate current sharing.

### A. Conventional Hierarchical Control

Fig. 5 shows the structure of conventional droop controller for a unit of DGUs with CPL, where droop mechanism adjusts the input voltage for each DGU based on the following expression:

$$v_{di} = v_{dc}^* - R_{di} i_{oi} \quad (23)$$

where  $R_{di}$  is the droop gain for DGU $i$  and can be expressed as follows:

$$R_{di} = \frac{\Delta v_{oi}}{i_{oi\_max}} \quad (24)$$

in which  $\Delta v_{oi}$  is acceptable voltage changes and  $i_{oi\_max}$  is maximum rating current of DGU $i$ .

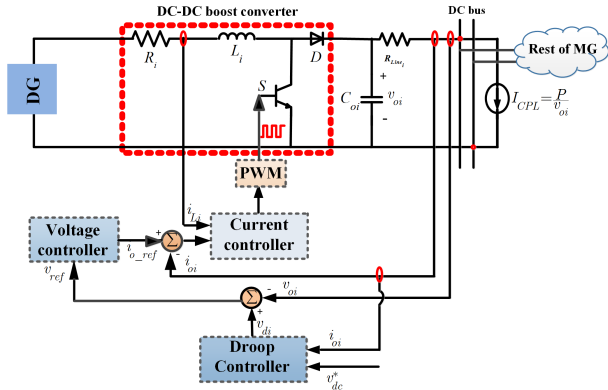


Fig. 5: Control diagram of conventional droop controller for DGU<sub>i</sub>.

### B. Decentralized Model Predictive Control

An optimal decentralized MPC is designed for each converter of the dc MG to guarantee appropriate current sharing and control of the dc bus voltage (see Fig. 6). As it is seen, the controller is implemented locally and no digital communication is utilized. The proposed DMPC provides optimal switching states for the dc-dc converter by solving an optimization problem using some real measurements, i.e., capacitor voltage and inductor current. In the provided solution, error is predicted-due to the nature of MPC controller- before applying the control signal to the converter, it uses a simple cost function to include the CS and VR control objectives. The following steps, as shown in the

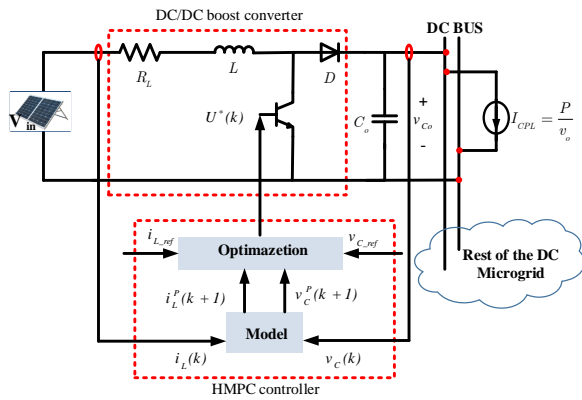


Fig. 6: Schematic of an optimal local controller based on DMPC controller for each dc-dc boost converter

flowchart of Fig. 7, are taken in order to design the proposed controller.

**Step 1. Prediction:** The first step to implement an MPC controller is building the system model. In this step, the required variables of the dc converter are measured to be used in the prediction process. After checking the status of switching states and the inductor current (see Fig. 4b), the perfect automatic mode is selected and the variable predictions are done consequently.

**Step 2. Cost function formulation:** Generally, the objective function  $J(k)$  is a penalties function in MPC which includes

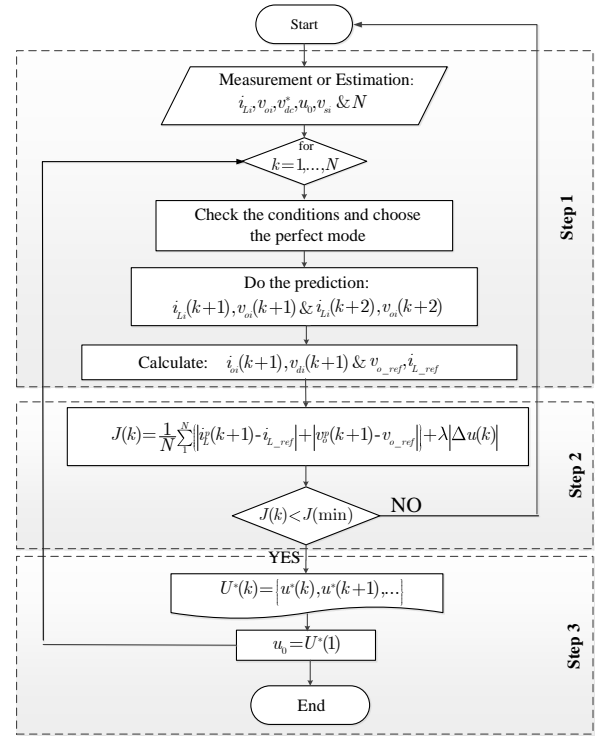


Fig. 7: Flowchart of the proposed controller

one term to penalize deviation from the desired trajectory and one term to penalize control efforts. The cost function is formulated based on the error of the predicted value ( $i_{Li}^p$  and  $v_{oi}^p$ ) of the state variables (inductive current and output voltage) with their desired reference value over the prediction horizon and optimal state switching ( $\Delta u(k)$ ) of the converter simultaneously, the cost functions of the MPCs for each DGU are proposed as:

$$J(k) = \frac{1}{N} \left\{ \sum_1^N (|i_{Li}^p(k+1) - i_{Li\_ref}| + |v_{oi}^p(k+1) - v_{oi\_ref}| + \lambda |\Delta u(k)|) \right\} \quad (25)$$

where,  $N$  is the prediction horizon,  $v_{oi\_ref}$  is voltage reference for DGU<sub>i</sub> which is equal to  $v_{dc}^*$ , and the initial value depends on the initial value of the output current in each unit, and  $i_{Li\_ref}$  is achieved using the power balance equation  $P_{in} = P_{out}$  and the desired current which can be calculated as follows:

$$P_{in} = v_{si} i_{Li} \quad , \quad P_{out} = P_{Load} \quad \Rightarrow \quad i_{Li\_des} = \frac{P_{Load}}{v_{si}} \quad (26)$$

To improve the transient of the output voltage, proportional term  $h$  is multiplied by the voltage error. Hence, the reference inductor current can be obtained as:

$$i_{Li\_ref} = i_{Li\_des} + h(v_{di} - v_{oi}) \quad (27)$$

where  $h \in \mathcal{R}^+$  is the small-ripple approximation for regulation of output voltage in steady state and adjusted voltage for each DGU is obtained as:

$$v_{di}(k+1) = v_{dc}^* - R_{di} i_{oi}(k+1) \quad (28)$$

and also, the difference of control signal, i.e., the error between two consecutive switching states is defined as:

$$\Delta u(k) = u(k) - u(k-1) \quad (29)$$

where  $\lambda > 0$  is the weighting factor which sets the trade-off between the inductor current/output voltage error. This parameter often considered to be a small value.

**Step 3. Optimization problem:** At each sample time, the following constraint optimization problem must be solved,

$$\begin{aligned} U^*(k) &= \arg \min J(k) \\ \text{Subj. to } &(15) \ \& \ (21) \end{aligned} \quad (30)$$

Minimizing the cost function results in a sequence in the form  $U^*$ , where  $U^*(k) = \{u^*(k), u^*(k+1), \dots\}$ . There exist  $2^N$  switching sequences and only its first element i.e.,  $u^*(k)$  is applied in each sampling time.

#### IV. REAL-TIME HIL RESULTS

Performance of the proposed DMPC is evaluated using the dc MG system shown in Fig. 2 including four DGUs interfaced with dc-dc boost converters connected to a CPL. The electrical and control parameters of the test system are listed in Table I. The dc MG test system augmented with the proposed control framework is implemented in OPAL-RT OP5600 as shown in Fig. 8. This allows us to verify the real-time effectiveness of the proposed DMPC. The detail configuration of the experimental platform is shown in Fig. 8(a). The converter based sources provides different ratings, i.e., the power rating of the DGU1 and DGU3 is double of the DGU2 and DGU4. Performance of the proposed controller is evaluated under different scenarios, and the results are compared with the conventional primary control.

TABLE I: Electrical and Control Parameters.

Electrical Parameters		
Parameter	Symbol	Value
The dimension of the state variable vector	$n$	2
The number of outputs	$q$	1
Input voltage	$v_{si}$	150 V
Voltage reference	$v_{dc}^*$	200 V
CPL	$P$	400 W
Filter inductance	$L_i$	450 $\mu$ H
Filter Capacitance	$C_{oi}$	220 $\mu$ F
Input resistance	$R_i$	0.01 $\Omega$
Line resistance	$R_{Line_i}$	0.3 $\Omega$
Control Parameters		
Sampling Time	$T_s$	2.5 $\mu$ s
Prediction horizon	$N$	3
Weighting factor	$\lambda$	0.01
Ripple approximation	$h$	0.7
Proportional gain of current loop	$K_{pI}$	3
Integral gain of current loop	$K_{iI}$	20
Proportional gain of voltage loop	$K_{pV}$	10
Integral gain of voltage loop	$K_{iV}$	200
Droop gain for DGU1,3	$R_{d1}, R_{d3}$	0.2
Droop gain for DGU2,4	$R_{d2}, R_{d4}$	0.4

##### A. Case Study 1: Load Step Change

Fig. 9 illustrates performance of the proposed DMPC in accurate power sharing and regulating voltage of the system under a step power load change in comparison with

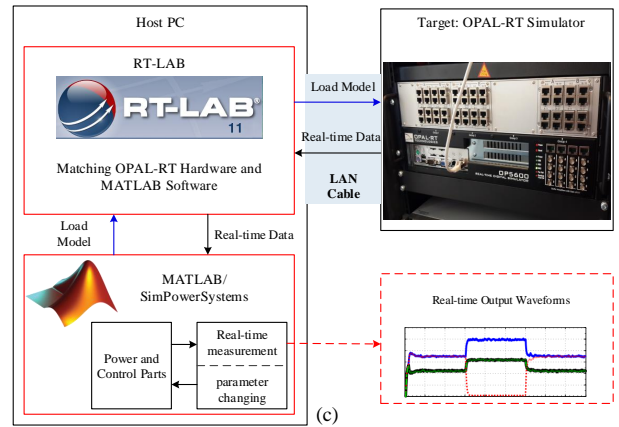
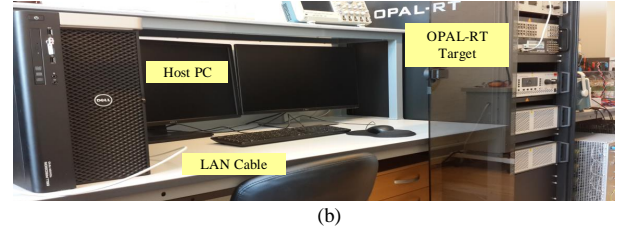
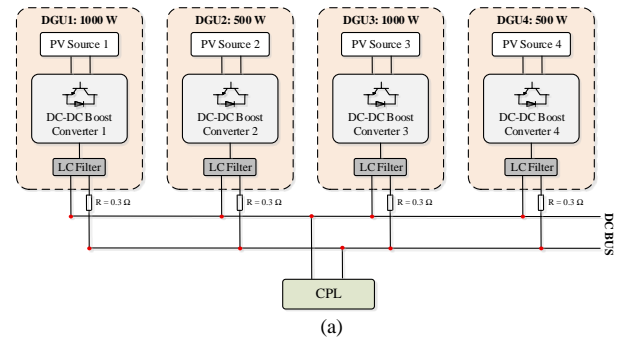


Fig. 8: Test bench of MG and implementation on real-time OPAL-RT: (a) schematic of the system configuration, (b) real-time experimental setup including the host PC, the OPAL-RT target and a LAN cable for networking, and (c) conceptual diagram of the DMPC real-time process.

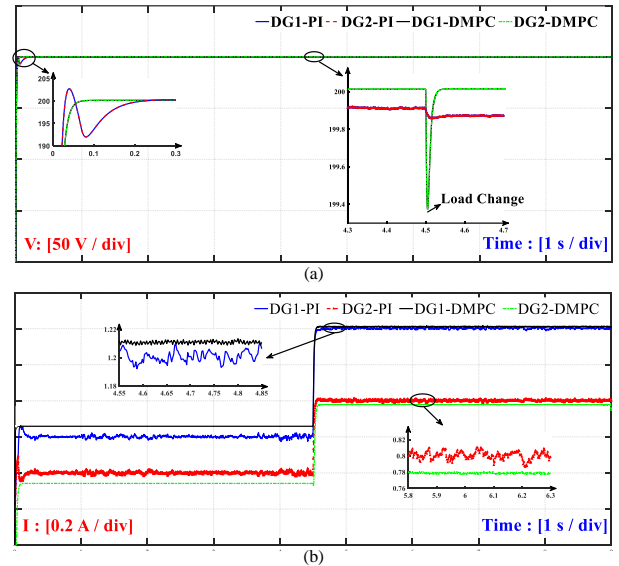


Fig. 9: Comparison of the proposed DMPC and the conventional droop control performance under CPL step change: (a) DG1 and DG2 voltage, and (b) current sharing among DGUs.



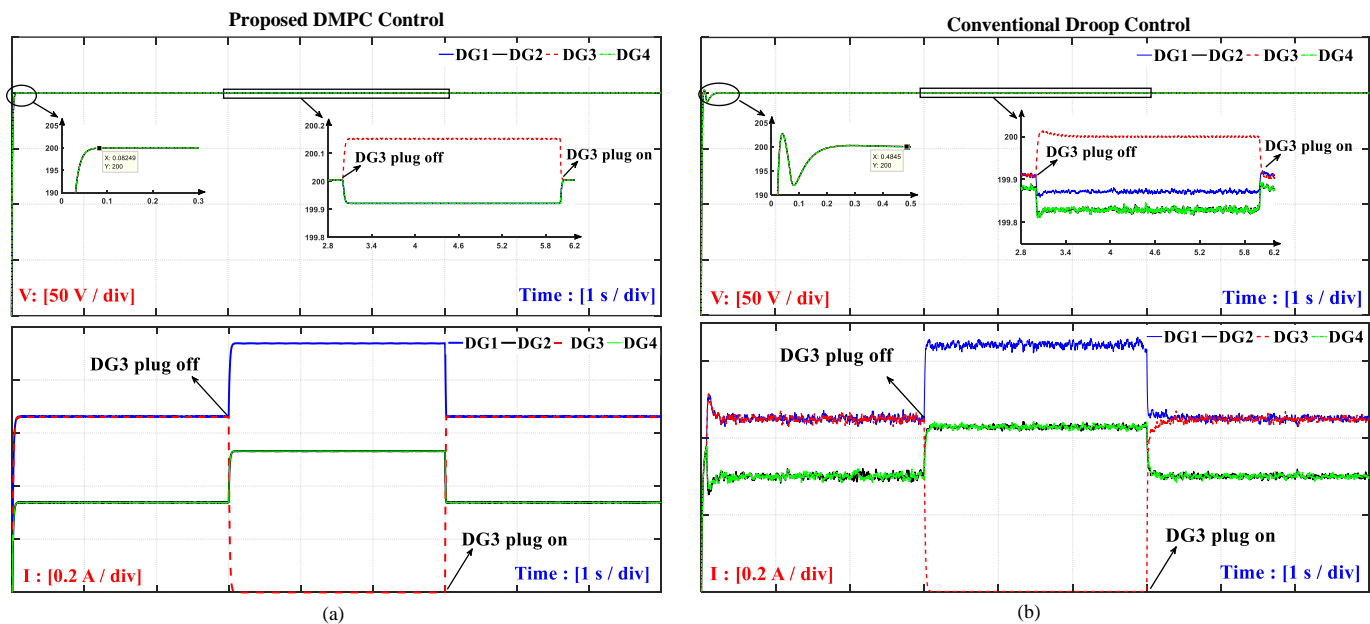


Fig. 10: PnP capability of the proposed DMPC versus the conventional primary (droop) control: (a) the proposed DMPC control, and (b) the conventional droop control.

the conventional primary control. Output power of the CPL connected to the system is stepped up from 400W to 800W at  $t = 4.5s$ . Clearly, current sharing and the dc-bus voltage are tightly controlled by using the proposed DMPC method. On the other hand, current sharing and the dc-bus voltage present large oscillations for the conventional droop control method. This demonstrates the excellent control performance of the proposed DMPC controller. The dc-bus voltage and output current of DG3 and DG4 are similar to that of DG1 and DG2 respectively, which is not shown here.

### B. Case Study 2: PnP operation of DGUs

Plug and play (PnP) capability of the DMPC controller is studied and shown in Fig. 10, where the results are compared with the conventional primary control, i.e., droop mechanism. It is assumed that DGU3 is plugged out from the system at  $t = 3s$  and it is plugged in at  $t = 6s$ . Fig. 10 shows a superior performance of the proposed controller for both transient and steady-state response. The voltage and current amplitudes in the proposed DMPC synchronize to the reference within approximately 0.08s, much faster than the settling time of 0.4s in the conventional method. The conventional droop control provides a slow response and high overshoot; therefore, it may not be suitable when the paralleled system must share nonlinear loads. On the other hand, the MPC controller has been able to achieve the control objectives with the fast response time and without any overshoot.

## V. CONCLUSION

This paper proposes a decentralized MPC to provide voltage regulation and current sharing of dc MGs interfaced with CPLs, taking the responsibility of conventional primary control. The proposed DMPC utilizes automatic model of the system for prediction used in the cost function. Optimum state

for switching is selected by the multi-objective cost function. Various case studies are done in OPAL-RT to evaluate the real-time performance of the proposed DMPC. In addition, the performance of the proposed DMPC is compared with conventional droop control. Real-time results verify the practical operation and effectiveness of the proposed method.

## REFERENCES

- [1] J. Chen, C. Wang, and J. Chen, "Investigation on the selection of electric power system architecture for future more electric aircraft," *IEEE Trans. Transp. Electrification*, vol. 4, no. 2, pp. 563–576, 2018.
- [2] E. R. M. M. T. A. J. E. Skjong, R. Volden and J. Cunningham, "Past, present, and future challenges of the marine vessels electrical power system," *IEEE Trans. Transp. Electrification*, vol. 2, no. 4, pp. 522–537, 2018.
- [3] T. Dragičević, X. Lu, J. C. Vasquez, and J. M. Guerrero, "Dc microgrid part i: A review of control strategies and stabilization techniques," *IEEE Trans. Power Electron.*, vol. 31, no. 7, pp. 4876–4891, 2015.
- [4] A. Emadi, A. Khaligh, C. H. Rivetta, and G. A. Williamson, "Constant power loads and negative impedance instability in automotive systems: definition, modeling, stability, and control of power electronic converters and motor drives," *IEEE Trans. Veh. Technol.*, vol. 55, no. 4, pp. 1112–1125, 2006.
- [5] M. Cespedes, L. Xing, and J. Sun, "Constant-power load system stabilization by passive damping," *IEEE Trans. Power Electron.*, vol. 26, no. 7, pp. 1832–1836, 2011.
- [6] A. M. Rahimi and A. Emadi, "Active damping in dc/dc power electronic converters: A novel method to overcome the problems of constant power loads," *IEEE Trans. Ind. Electron.*, vol. 56, no. 5, pp. 1428–1439, 2009.
- [7] A. M. Rahimi, G. A. Williamson, and A. Emadi, "Loop-cancellation technique: A novel nonlinear feedback to overcome the destabilizing effect of constant-power loads," *IEEE Trans. Veh. Technol.*, vol. 59, no. 2, pp. 650–661, 2010.
- [8] Z. Qu, S. Ebrahimi, N. Amiri, J. Jatskevich, and A. Pizniur, "Adaptive control method for stabilizing dc distribution systems with constant-power loads based on tunable active damping," in *2018 IEEE 19th Workshop on Control and Modeling for Power Electronics (COMPEL)*. IEEE, 2018, pp. 1–6.
- [9] F. Gao, S. Bozhko, A. Costabeber, C. Patel, P. Wheeler, C. I. Hill, and G. Asher, "Comparative stability analysis of droop control approaches in voltage-source-converter-based dc microgrids," *IEEE Trans. Power Electron.*, vol. 32, no. 3, pp. 2395–2415, 2016.
- [10] A. Kwasinski and C. N. Onwuchekwa, "Dynamic behavior and stabilization of dc microgrids with instantaneous constant-power loads," *IEEE Trans. Power Electron.*, vol. 26, no. 3, pp. 822–834, 2010.

- [11] X. Feng, J. Liu, and F. C. Lee, "Impedance specifications for stable dc distributed power systems," *IEEE Trans. Power Electron.*, vol. 17, no. 2, pp. 157–162, 2002.
- [12] X. Zhang, D. M. Vilathgamuwa, K.-J. Tseng, B. S. Bhangu, and C. J. Gajanayake, "Power buffer with model predictive control for stability of vehicular power systems with constant power loads," *IEEE Trans. Power Electron.*, vol. 28, no. 12, pp. 5804–5812, 2012.
- [13] A. M. Rahimi and A. Emadi, "Active damping in dc/dc power electronic converters: A novel method to overcome the problems of constant power loads," *IEEE Trans. Ind. Electron.*, vol. 56, no. 5, pp. 1428–1439, 2009.
- [14] T. Dragičević, "Dynamic stabilization of dc microgrids with predictive control of point-of-load converters," *IEEE Trans. Power Electron.*, vol. 33, no. 12, pp. 10872–10884, 2018.
- [15] V. Nasirian, S. Moayedi, A. Davoudi, and F. L. Lewis, "Distributed cooperative control of dc microgrids," *IEEE Trans. Power Electron.*, vol. 30, no. 4, pp. 2288–2303, 2014.
- [16] P. Monica and M. Kowsalya, "Control strategies of parallel operated inverters in renewable energy application: A review," *newable and Sustainable Energy Reviews*, vol. 65, no. 3, pp. 885–901, 2016.
- [17] D. B. J. V. F. Chen, R. Burgos and J. M. Guerrero, "Investigation of nonlinear droop control in dc power distribution systems: Load sharing, voltage regulation, efficiency and stability," *IEEE Transactions on Power Electronics*, 2019.
- [18] Y. G. P. Prabhakaran and V. Agarwal, "Novel nonlinear droop control techniques to overcome the load sharing and voltage regulation issues in dc microgrid," *IEEE Trans. Power Electron.*, vol. 33, no. 5, pp. 4477–4487, 2018.
- [19] H. M. S. Peyghami, P. Davari and F. Blaabjerg, "Decentralized droop control in dc microgrids based on a frequency injection approach," *IEEE Transactions on Smart Grid*, 2019.
- [20] F. Gao, S. Bozhko, A. Costabeber, C. Patel, P. Wheeler, C. I. Hill, and G. Asher, "Comparative stability analysis of droop control approaches in voltage-source-converter-based dc microgrids," *IEEE Transactions on Power Electronics*, vol. 32, no. 3, pp. 2395–2415, 2016.
- [21] S. Augustine, M. K. Mishra, and N. Lakshminarasamma, "Adaptive droop control strategy for load sharing and circulating current minimization in low-voltage standalone dc microgrid," *IEEE Trans. Sustain. Energy*, vol. 6, no. 1, pp. 132–141, 2014.
- [22] E. Shehata, J. Thomas, R. Mostafa, and M. Ghalib, "An improved droop control for a low voltage dc microgrid operation," in *2018 Twentieth International Middle East Power Systems Conference (MEPCON)*. IEEE, 2018, pp. 850–855.
- [23] S. Augustine, M. K. Mishra, and N. Lakshminarasamma, "Adaptive droop control strategy for load sharing and circulating current minimization in low-voltage standalone dc microgrid," *IEEE Transactions on Sustainable Energy*, vol. 6, no. 1, pp. 132–141, 2014.
- [24] A. Khorsandi, M. Ashourloo, H. Mokhtari, and R. Irvani, "Automatic droop control for a low voltage dc microgrid," *IET Generation, Transmission & Distribution*, vol. 10, no. 1, pp. 41–47, 2016.
- [25] L. Cheng, P. Acuna, R. P. Aguilera, J. Jiang, S. Wei, J. E. Fletcher, and D. D. Lu, "Model predictive control for dc–dc boost converters with reduced-prediction horizon and constant switching frequency," *IEEE Trans. Power Electron.*, vol. 33, no. 10, pp. 9064–9075, 2017.
- [26] Y. Du, J. Wu, S. Li, C. Long, and S. Onori, "Coordinated energy dispatch of autonomous microgrids with distributed mpc optimization," *IEEE Transactions on Industrial Informatics*, 2019.
- [27] T. Dragičević, "Model predictive control of power converters for robust and fast operation of ac microgrids," *IEEE Transactions on Power Electronics*, vol. 33, no. 7, pp. 6304–6317, 2017.
- [28] K. Liu, T. Liu, Z. Tang, and D. J. Hill, "Distributed mpc-based frequency control in networked microgrids with voltage constraints," *IEEE Transactions on Smart Grid*, 2019.
- [29] M. Yu, Y. Wang, and Y. Li, "Hierarchical control of dc microgrid based on model predictive controller," in *IECON 2016-42nd Annual Conference of the IEEE Industrial Electronics Society*. IEEE, 2016, pp. 4139–4144.
- [30] S. Xiao, M. B. Shadmand, and R. S. Balog, "Model predictive control of multi-string pv systems with battery back-up in a community dc microgrid," in *2017 IEEE Applied Power Electronics Conference and Exposition (APEC)*. IEEE, 2017, pp. 1284–1290.
- [31] N. Vafamand, M. H. Khooban, T. Dragičević, and F. Blaabjerg, "Networked fuzzy predictive control of power buffers for dynamic stabilization of dc microgrids," *IEEE Transactions on Industrial Electronics*, vol. 66, no. 2, pp. 1356–1362, 2018.
- [32] X. Zhang, B. Wang, U. Manandhar, H. B. Gooi, and G. Foo, "A model predictive current controlled bidirectional three-level dc/dc converter for

hybrid energy storage system in dc microgrids," *IEEE Transactions on Power Electronics*, 2018.

- [33] M. M. Mardani, M. H. Khooban, A. Masoudian, and T. Dragičević, "Model predictive control of dc–dc converters to mitigate the effects of pulsed power loads in naval dc microgrids," *IEEE Transactions on Industrial Electronics*, vol. 66, no. 7, pp. 5676–5685, 2018.
- [34] P. Karamanakos, T. Geyer, and S. Manias, "Direct model predictive current control strategy of dc–dc boost converters," *IEEE J. Emerg. Sel. Top. in Power Electron.*, vol. 1, no. 4, pp. 337–346, 2013.
- [35] Z. Karami, Q. Shafiee, Y. Batmani, and H. Bevrani, "On the design of suboptimal controller for dc microgrids with cpl," *Energy Procedia*, vol. 141, pp. 611–618, 2017.



**Zeinab Karami** (S'16) is a Researcher at the Smart/Micro Grids Research Center (SMGRC), University of Kurdistan, Sanandaj, Iran. She received her B.S. and M.S. degrees from University of Kurdistan, Sanandaj, Iran, in 2015 and 2017, respectively. Her main research interests include microgrid stability and control, model predictive, nonlinear, optimal and robust control for application of power electronics in distributed systems.



**Qobad Shafiee** (S'13-M'15-SM'17) received PhD degree in electrical engineering from the Department of Energy Technology, Aalborg University (Denmark) in 2014. He is currently an Assistant Professor, Director of International Relations, and Program Co-Leader of the Smart/Micro Grids Research Center at the University of Kurdistan, Sanandaj, Iran, where he was a lecturer from 2007 to 2011. In 2014, he was a Visiting Scholar with the Electrical Engineering Department, the University of Texas at Arlington, Arlington, TX, USA. He was a Post-Doctoral Fellow with the Department of Energy Technology, Aalborg University in 2015. His current research interests include modeling, energy management, control of power electronics-based systems and microgrids, and model predictive and optimal control of modern power systems.



**Yousef Khayat** (S'16) received the B.Sc. degree from Urmia University, Urmia, Iran, and the M.Sc. degree (with Hons.) from Iran University of Science and Technology (IUST), Tehran, Iran, both in Electrical Engineering in 2012 and 2014, respectively. He is working toward the Ph.D. degree in control of power systems at the University of Kurdistan, Iran. He is also currently a Ph.D. Visiting Student with Aalborg University, Aalborg, Denmark. His research interests include Microgrid dynamics and control, robust, predictive and nonlinear control application of power electronics in distributed systems.



**Meysam Yaribeygi** received the B.S. and M.S. degrees in electrical engineering from University of Kurdistan, Sanandaj, Iran, in 2015 and K.N. Toosi University of Technology, Tehran, Iran, in 2017, respectively. He is currently a research engineer at SINA Innovative Communications Systems. His research interests focus on optical network control plane and resource allocation, optimization, and microgrid communications.



**Tomislav Dragievi** (S'09-M'13-SM'17) received the M.Sc. and the industrial Ph.D. degrees in Electrical Engineering from the Faculty of Electrical Engineering, Zagreb, Croatia, in 2009 and 2013, respectively. From 2013 until 2016 he has been a Postdoctoral research associate at Aalborg University, Denmark. From March 2016 he is an Associate Professor at Aalborg University, Denmark where he leads an Advanced Control Lab. He made a guest professor stay at Nottingham University, UK during spring/summer of 2018. His principal field of interest is design and

control of microgrids, and application of advanced modeling and control concepts to power electronic systems. He has authored and co-authored more than 180 technical papers (more than 80 of them are published in international journals, mostly IEEE Transactions) in his domain of interest, 8 book chapters and a book in the field. He serves as Associate Editor in the IEEE TRANSACTIONS ON INDUSTRIAL ELECTRONICS, in IEEE Emerging and Selected Topics in Power Electronics and in IEEE Industrial Electronics Magazine. Dr. Dragievi is a recipient of the Konar prize for the best industrial PhD thesis in Croatia, and a Robert Mayer Energy Conservation award.



**Hassan Bevrani** (S'90-M'04-SM'08) received PhD degree in electrical engineering from Osaka University (Japan) in 2004. He is a full professor and the program leader of Smart/Micro Grids Research Center (SMGRC) at the University of Kurdistan (UOK). During 2016-2019, he has been the UOK vice chancellor for Research and Technology. Over the years, he has worked as senior research fellow and visiting professor with Osaka University, Kumamoto University (Japan), Queensland University of Technology (Australia), Kyushu Institute of Tech-

nology (Japan), Centrale Lille (France), and Technical University of Berlin (Germany). Currently, he is a visiting professor in Osaka University. Prof. Bevrani is the author of 6 international books, 15 book chapters, and more than 300 journal/conference papers. His current research interests include smart grid operation and control, power systems stability and optimization, Microgrid dynamics and control, and Intelligent/robust control applications in power electric industry.